Cluster-model calculation of quadrupole effects in pion scattering from ^{7}Li

Naoko Nose
Department of Physics, Nara Women's University, Nara 630, Japan

Kenji Kume*
TRIUMF, 4004 Wesbrook Mall, Vancouver, British Columbia, Canada V6T 2A3

Shinichiro Yamaguchi
Research Center of Nuclear Physics, Osaka University, Ibaraki 567, Japan
(Received 6 December 1993)

We have studied the quadrupole effects in pion elastic and inelastic scattering from ^{7}Li. A single channel α-t cluster model is used to calculate the wave function for the ground and the first excited states of ^{7}Li. The quadrupole effects are shown to be appreciably large in pion-^{7}Li elastic scattering. We also calculated the second-rank tensor polarization and compared it with the recent experimental data.

PACS number(s): 21.60.Gx, 25.80.Dj, 25.80.Ek, 27.20.+n

I. INTRODUCTION

Although pion-nucleus scattering has been extensively studied over the past two decades, these studies were mainly concerned with spinless nuclei. Recently, however, the experiments from polarized nuclei have been carried out and the interest has grown for pion scattering from nuclei with nonzero spin [1–5]. In the elastic scattering from spin-$\frac{1}{2}$ nuclei, the asymmetry comes from the interference between pion-nucleus spin-flip and spin-nonflip amplitudes and the spin effects have been discussed. For the nuclear targets having spin larger than one, various multipole scattering effects become to be important. In particular, for the case of deformed nuclei, we expect that the spin-nonflip quadrupole scattering largely affects not only the pion scattering cross section but also the polarization observables. The deformation effects are expected to be appreciable in the second-rank tensor polarization. Based on this expectation, an experiment using the pion single-charge-exchange reaction was carried out on an aligned ^{165}Ho target leading to its isobaric analog state [6]. The neutron deformation parameter was extracted from the asymmetry at forward direction.

The main purpose of this paper is to investigate the quadrupole effects on the elastic and inelastic scattering of pion from deformed nuclei. In order to examine the various possibilities in pion scattering, it is interesting to study to what extent the quadrupole deformation affects the elastic and inelastic scattering. For this purpose, the ^{7}Li nucleus is well suited since its structure is thoroughly studied through electromagnetic interaction and we can minimize the ambiguities coming from nuclear structure. Furthermore, experimental data are available at 164 MeV [7] and at 143 MeV [8]. Very recently, a pion scattering experiment on polarized ^{7}Li has been carried out at the Paul Scherrer Institute (PSI) [9].

Several theoretical calculations on pion-^{7}Li scattering were done, but these are based on a simple model; the collective model [8] or the shell model [10]. As for the structure of ^{7}Li, however, many theoretical studies [11–17] showed that the electromagnetic properties of ground and first excited states of ^{7}Li are well understood from the viewpoint of the cluster structure and that a large quadrupole deformation of these states is attributed to the dominant α-t cluster configuration. These structures are well described by the resonating-group method (RGM). Especially, the electromagnetic quantities of ^{7}Li at $q \leq 2$ fm^{-1} are well described by the RGM wave function [17]. Recently, a more elaborate calculation has been carried out [18], where the effects of the additional configurations are considered and it was shown that the α-t component dominates in the ground and first excited states while the other components give important contribution to higher excited states.

In this paper, we derive the wave function of the ground and the first excited states of ^{7}Li with the single-channel α-t RGM. By the use of these wave functions, we calculate the ground-state and transition densities. As a monopole part of the pion-nucleus optical potential, we use the semiphenomenological potential by Stricker *et al.* [19–21] (MSU potential) for spherical nucleus with the parameters B_0 and C_0 for ρ^2 terms determined by Gmitro *et al.* [22]. The multipole part of the pion-^{7}Li optical potential is constructed by folding the pion-nucleon t matrix [23] under the first-order approximation. With this pion-nucleus optical potential, we calculated the quadrupole effects in the elastic scattering of pion on ^{7}Li. The inelastic scattering cross section leading to the first excited state is also calculated under distorted-wave impulse approximation (DWIA).

We also calculated the second-rank tensor polarization

*On leave from Department of Physics, Nara Women's University, Nara 630 Japan.

Θ_{zz} in pion scattering from polarized ^{7}Li and compared with the recent experimental data. Due to its large deformation, the absolute value of the second-rank tensor polarization takes large absolute values which is in contrast to the rather small vector analyzing powers observed in pion scattering from polarized spin-$\frac{1}{2}$ nuclei [1,2,4]. The vector polarization iT_{11} is also measured for pion-^{7}Li scattering and is shown to be fairly small [9]. Because the various multipole components in spin-nonflip and spin-flip pion-nucleus amplitudes interfere, we feel it better to consider the dominant quadrupole effects first: scattering cross section and second-rank tensor polarization. We do not discuss the vector polarization iT_{11} in the present paper.

In Sec. II, we describe the α-t cluster model. In order to calculate the ground-state densities and transition form factors, we applied the complex generator-coordinate method (GCM) and correctly eliminated the spurious component of the center-of-mass motion in the cluster wave function. We showed the details of the technique used to calculate the multipole densities. In Sec. III, we discuss the pion elastic and inelastic scattering from ^{7}Li. We extend the pion-nucleus optical potential to the case of the target nucleus with nonzero spin. We show that the coupling of the pion partial wave induced by the quadrupole deformation plays an important role for the elastic scattering. The inelastic-scattering cross section leading to the first excited state ^{7}Li($\frac{3}{2}^- \rightarrow \frac{1}{2}^-$:0.478 MeV) is calculated under DWIA and is compared with the experimental data. The averaged second-rank tensor polarization leading to the final ground and first excited states are shown and are compared with the recent experimental data. We summarize the results in Sec. IV.

II. CLUSTER-MODEL CALCULATION

A. Wave function of ^{7}Li

For the ground and the first excited states of ^{7}Li, we employ the RGM wave functions. As mentioned in Sec. I, the ground and the first excited states can be well described by the α-t cluster model. The internal wave functions of α and t are assumed to be those of the harmonic-oscillator shell model. The oscillator-size parameters for α and t are determined so as to reproduce the rms charge radii and are given as $\nu_\alpha = 0.546$ fm^{-2} and $\nu_t = 0.413$ fm^{-2}. As an effective interaction we employ the Volkov No. 2 force [24]. The Majorana parameter m is determined so as to reproduce the rms charge radius of the ^{7}Li; $m = 0.585$. We neglected the spin-orbit and the Coulomb interactions since these forces have little effect on the wave function of ^{7}Li.

Table I shows the rms charge radius, quadrupole moment of the ground state, and $B(E2{:}\frac{3}{2}^- \rightarrow \frac{1}{2}^- \uparrow)$. Figure 1 shows the longitudinal form factors. In the present calculation, proton and neutron form factors are taken from Ref. [31]. Similar to the results by Kajino *et al.* [17], we can see that the α-t cluster model reproduces well the experimental values of these electromagnetic quantities. The longitudinal form factors are well described at the momentum transfer less than 2 fm^{-1} which is sufficient for our purpose since we are concerned with the pion scattering below (3.3) resonance. It is noted that the n-^{6}Li configuration, which is neglected here, only slightly reduces the absolute value of the $C2$ form factor as was shown in Ref. [18].

TABLE I. The results of the energy level, rms charge radius, and the quadrupole moment for the ground state of ^{7}Li calculated with cluster model described in the text. In the last row, we show the reduced $E2$ transition rate to the first excited state. In the last column, the experimental values are listed which are taken from Refs. [25–29].

		Experiment
Energy level (MeV)	−2.789	-2.467 ($\frac{3}{2}^-$)[a]
		-1.989 ($\frac{1}{2}^-$)[a]
$\sqrt{\langle r_c^2 \rangle}$ (fm)	2.55	2.55±0.07[b]
Q (fm^2)	−4.454	|3.8±1.1|[b]
		−4.1[c]
		−4.44[d]
$B(E2;\uparrow)$ (e^2fm^4)	9.868	7±4[b]
		8.3±0.7[e]

[a]Reference [25].
[b]Reference [26].
[c]Reference [27].
[d]Reference [28].
[e]Reference [29].

We examined the dependence on the choice of the various input parameters. Instead of reproducing the rms radii of α and t, we adopted the saturation condition for each cluster to determine their size parameters. In this case the oscillator-size parameters are $\nu_\alpha = 0.524$ fm^{-2} and $\nu_t = 0.391$ fm^{-2} with Volkov No. 2. We also examined the Hasegawa-Nagata (HN) effective interaction [32]. The results are, however, quite insensitive to the choice of those input parameters. Therefore, we use the ^{7}Li wave function derived with the parameters $\nu_\alpha = 0.546$ fm^{-2}, $\nu_t = 0.413$ fm^{-2}, and $m = 0.585$ with the Volkov-2 effective interaction.

B. Ground-state and transition densities

In the practical calculation of the ground-state and transition densities, we used the complex GCM technique [33]. In this subsection, we briefly explain this method which is numerically accurate and probably wastes the least computational time. The symbols A and B repre-

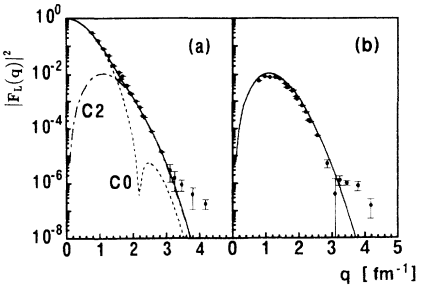

FIG. 1. Longitudinal electromagnetic form factors of ^{7}Li. (a) Ground state, (b) first excited state ^{7}Li($\frac{1}{2}^-$:0.478 MeV). The results are obtained with the RGM wave function. The experimental data are taken from Ref. [30].

sent the mass numbers of the two clusters and, at the same time, specify the clusters themselves. In order to calculate the elastic- and inelastic-scattering cross sections, we have to calculate the ground-state and transition matrix elements of the following density operators:

$$\left\{ \begin{matrix} \hat{\rho}^{(k)}(\mathbf{r}) \\ \hat{\boldsymbol{\rho}}^{(k)}(\mathbf{r}) \end{matrix} \right\} = \sum_j \left\{ \begin{matrix} 1 \\ \boldsymbol{\sigma}_j \end{matrix} \right\} \tau_3^{(k)}(j) \delta(\mathbf{r} - \tilde{\mathbf{r}}_j) \ , \tag{1}$$

where $\tilde{\mathbf{r}}_j$ is the relative coordinate of jth nucleon from the center of mass of the nucleus

$$\tilde{\mathbf{r}}_j = \mathbf{r}_j - \frac{\sum_{i=1}^{A} \mathbf{r}_i}{A+B} \ . \tag{2}$$

To be specific, we show how to calculate the transition density $\rho_{fi}^{(0)}(\mathbf{r})$ which is a matrix element of the operator $\hat{\rho}^{(0)}(\mathbf{r})$ in Eq. (1). The calculation of the other operators are the same. For simplicity, we omit the isospin indices in this subsection.

First, we expand the α-t relative wave function $\psi_{lm}^{(J)}(\mathbf{R})$ with the harmonic-oscillator basis

$$\psi_{lm}^{(J)}(\mathbf{R}) = \sum_N C_{Nl}^{(J)} \psi_{Nlm}(\mathbf{R}; \gamma) \ , \tag{3}$$

where γ is the oscillator-size parameter. With this expansion, the transition density $\rho_{fi}(\mathbf{r})$ can be written as

$$\begin{aligned} \rho_{fi}(\mathbf{r}) &= \langle [[\phi_\alpha^{\rm int} \otimes \phi_t^{\rm int}]_{S_f} \otimes \psi_{l_f}^{(J_f)}]_{J_f M_f} | \hat{\rho}(\mathbf{r}) | \mathcal{A}[[\phi_\alpha^{\rm int} \otimes \phi_t^{\rm int}]_{S_i} \otimes \psi_{l_i}^{(J_i)}]_{J_i M_i} \rangle \\ &= \sum (S_f l_f S_{zf} m_f | J_f M_f)(S_i l_i S_{zi} m_i | J_i M_i)(C_{N_f l_f}^{(J_f)})^* C_{N_i l_i}^{(J_i)} \langle S_f S_{zf} N_f l_f m_f | \hat{\rho}(\mathbf{r}) | S_i S_{zi} N_i l_i m_i \rangle \ , \end{aligned} \tag{4}$$

where $\phi_\alpha^{\rm int}$ and $\phi_t^{\rm int}$ are the internal wave functions of α and t and $\mathcal{A}$ is the antisymmetrizer. Then the problem is how to calculate the following matrix elements in harmonic-oscillator basis:

$$\langle S_f S_{zf} N_f l_f m_f | \hat{\rho}(\mathbf{r}) | S_i S_{zi} N_i l_i m_i \rangle = \langle [\phi_\alpha^{\rm int} \otimes \phi_t^{\rm int}]_{S_f S_{zf}} \psi_{N_f l_f m_f}(\gamma) | \hat{\rho}(\mathbf{r}) | \mathcal{A}[[\phi_\alpha^{\rm int} \otimes \phi_t^{\rm int}]_{S_i S_{zi}} \psi_{N_i l_i m_i}(\gamma)] \rangle \ . \tag{5}$$

In order to do this, we use the Bargmann-transformation kernel given by

$$\Gamma_\gamma(\mathbf{R}, \mathbf{Z}) = \left(\frac{\gamma}{\pi}\right)^{3/4} \exp\left(-\frac{\gamma}{2}(\mathbf{R} - \sqrt{2/\gamma}\mathbf{Z})^2 + \tfrac{1}{2}\mathbf{Z}^2\right) \ . \tag{6}$$

We define the complex GCM matrix element as follows and it can be expanded by using the harmonic-oscillator decomposition of the Bargmann-transformation kernel

$$\begin{aligned} &\langle [\phi_\alpha^{\rm int} \otimes \phi_t^{\rm int}]_{S_f S_{zf}} \Gamma_\gamma(\mathbf{Z}) | \hat{\rho}(\mathbf{r}) | \mathcal{A}[[\phi_\alpha^{\rm int} \otimes \phi_t^{\rm int}]_{S_i S_{zi}} \Gamma_\gamma(\mathbf{Z}')] \rangle \\ &\qquad = \sum_{N_f l_f m_f} \sum_{N_i l_i m_i} [f_{N_f l_f m_f}(\mathbf{Z})]^* \langle S_f S_{zf} N_f l_f m_f | \hat{\rho}(\mathbf{r}) | S_i S_{zi} N_i l_i m_i \rangle f_{N_i l_i m_i}(\mathbf{Z}') \ , \end{aligned} \tag{7}$$

where $f_{Nlm}(\mathbf{Z})$ is the harmonic-oscillator wave function in Bargmann representation. The matrix elements in Eq. (5) can be obtained as the expansion coefficients of the complex GCM matrix elements. To calculate the complex GCM matrix elements, we introduce the GCM wave function

$$\Psi_{SSz}(\mathbf{X}_A, \mathbf{X}_B) = \frac{1}{\sqrt{(A+B)!}} \mathcal{A}[\phi_1^{(A)}(\mathbf{r}_1 - \mathbf{X}_A), \ldots, \phi_A^{(A)}(\mathbf{r}_A - \mathbf{X}_A), \phi_{A+1}^{(B)}(\mathbf{r}_{A+1} - \mathbf{X}_B), \ldots, \phi_{A+B}^{(B)}(\mathbf{r}_{A+B} - \mathbf{X}_B)]_{SS_z} \ , \tag{8}$$

where $\mathbf{X}_A$ and $\mathbf{X}_B$ are the generator coordinates specifying the location of two clusters. $\phi_i^{(A)}$ and $\phi_i^{(B)}$ are the single-particle wave functions of harmonic-oscillator type. Using the above wave function, the real GCM matrix element of the density operator is given by

$$\rho_{fi}(\mathbf{X}_A, \mathbf{X}_B; \mathbf{X}'_A, \mathbf{X}'_B; \mathbf{r}) = \langle \Psi_{S_f S_{zf}}(\mathbf{X}_A, \mathbf{X}_B) | \hat{\rho}(\mathbf{r}) | \Psi_{S_i S_{zi}}(\mathbf{X}'_A, \mathbf{X}'_B) \rangle \ . \tag{9}$$

This can be easily calculated by noting that the operator $\hat{\rho}(\mathbf{r})$ can be written as

$$\hat{\rho}(\mathbf{r}) = \frac{1}{(2\pi)^3} \int d\mathbf{q} \prod_{j=1}^{A+B} \exp\left(-i\mathbf{q} \cdot \frac{\mathbf{r}_j}{A+B}\right) \sum_{j=1}^{A+B} e^{i\mathbf{q}\cdot(\mathbf{r}_j - \mathbf{r})} \ , \tag{10}$$

and the exponential $\exp[-i\mathbf{q} \cdot \mathbf{r}_j/(A+B)]$ appearing in above equation can be absorbed into the single-particle wave functions in bra- or ket-state.

In the case that the oscillator-size parameters of the clusters are different, we have to explicitly eliminate the spurious center-of-mass component in the GCM matrix element which couples the center-of-mass motion to the intercluster relative motion. In order to do this, it is sufficient to integrate with respect to the center-of-mass generator coordinate in the bra-state

$$\rho_{fi}(\mathbf{X},\mathbf{X}';\mathbf{r}) = \left(\frac{A\nu_A + B\nu_B}{4\pi}\right)^{3/2} \int d\mathbf{X}_G \rho_{fi}(\mathbf{X}_A,\mathbf{X}_B;\mathbf{X}'_A,\mathbf{X}'_B;\mathbf{r}) \,, \tag{11}$$

where $\mathbf{X}=\mathbf{X}_B - \mathbf{X}_A$ and $\mathbf{X}_G = (A\mathbf{X}_A + B\mathbf{X}_B)/(A+B)$, and the same for $\mathbf{X}'$ and $\mathbf{X}'_G$. After the integration in Eq. (11), the GCM marix element does not depend on the generator coordinate $\mathbf{X}'_G$ and is free from the spurious center-of-mass component.

From this real GCM, we can immediately obtain the complex GCM matrix elements by the suitable replacement of $(\mathbf{X},\mathbf{X}')$ by complex variables $(\mathbf{Z},\mathbf{Z}')$ [33].

For the α-t system, the complex GCM matrix element can be generally written as

$$\rho_{fi}(\mathbf{Z}^*,\mathbf{Z}';\mathbf{r})\exp\left(\frac{\mathbf{Z}^{*2}+\mathbf{Z}'^2}{2}\right) = \sum_j g_j \exp[-a_j\mathbf{Z}^{*2} - b_j\mathbf{Z}'^2 + c_j\mathbf{Z}^*\cdot\mathbf{Z}' + d_j\mathbf{Z}^*\cdot\mathbf{r} + e_j\mathbf{Z}'\cdot\mathbf{r} - f_j\mathbf{r}^2] \,, \tag{12}$$

where a_j, b_j, and f_j are positive constants. Note that the coefficients g_j depend not only on the type of the density operator but also on the spin variables (S_i, S_{zi}) and (S_f, S_{zf}). The exponential part of the right-hand side of Eq. (12) can be expanded as

$$\begin{aligned}
\exp[-a\mathbf{Z}^{*2} - b\mathbf{Z}'^2 + c\mathbf{Z}^*\cdot\mathbf{Z}' + d\mathbf{Z}^*\cdot\mathbf{r} + e\mathbf{Z}'\cdot\mathbf{r} - f\mathbf{r}^2] = {} & \left(\frac{4\pi\sqrt{ab}}{|ed|}\right)^{3/2} \exp\left[-\left(f - \frac{d^2}{8a} - \frac{e^2}{8b}\right)r^2\right] \\
& \times \sum_{N_1 l_1 m_1} \psi^*_{N_1 l_1 m_1}\left(\mathbf{r};\frac{d^2}{4a}\right)\{f_{N_1 l_1 m_1}[\mathrm{sgn}(d)\sqrt{2a}\mathbf{Z}]\}^* \\
& \times \sum_{N_2 l_2 m_2} \psi_{N_2 l_2 m_2}\left(\mathbf{r};\frac{e^2}{4b}\right) f_{N_2 l_2 m_2}[\mathrm{sgn}(e)\sqrt{2b}\mathbf{Z}'] \\
& \times \sum_{N_3 l_3 m_3} [f_{N_3 l_3 m_3}(\sqrt{|c|}\mathbf{Z})]^* f_{N_3 l_3 m_3}[\mathrm{sgn}(c)\sqrt{|c|}\mathbf{Z}'] \,,
\end{aligned} \tag{13}$$

where $\mathrm{sgn}(d) = d/|d|$ indicates the sign of "d," etc. Comparing the harmonic-oscillator expansion of the complex GCM in Eq. (7), we obtain the following expression for the transition densities calculated with the cluster wave function:

$$\begin{aligned}
&\langle S_f S_{zf} N_f l_f m_f|\hat{\rho}(\mathbf{r})|S_i S_{zi} N_i l_i m_i\rangle \\
&= 4\pi \sum_j g_j \left(\frac{\sqrt{a_j b_j}}{|d_j e_j|}\right)^{3/2} \exp\left[-\left(f_i - \frac{d_j^2}{8a_j} - \frac{e_j^2}{8b_j}\right)r^2\right] \\
&\quad \times \sum_{N=0}^{\min\{N_f,N_i\}} \sum_{l=(0,1)}^{N_f-N} \sum_{l'=(0,1)}^{N_i-N} \sum_{l''=(0,1)}^{N} (-)^{(l_i+l_f+l+l')/2} \\
&\quad \times [\mathrm{sgn}(e)]^{l'}[\mathrm{sgn}(d)]^l R_{N_i-N,l'}\left(r;\frac{e_j^2}{4b_j}\right) R_{N_f-N,l}\left(r;\frac{d_j^2}{4a_j}\right) \\
&\quad \times \left[\frac{(N_f+l_f+1)!!(N_f-l_f)!!(N_i+l_i+1)!!(N_i-l_i)!!}{(N_i-N+l'+1)!!(N_i-N-l')!!(N_f-N+l+1)!!(N_f-N-l)!!}\right]^{1/2} \\
&\quad \times \frac{(2l+1)(2l'+1)(2l''+1)}{(N+l''+1)!!(N-l'')!!} (l'l''00|l_i 0)(ll''00|l_f 0)(2b_j)^{N_i-N/2}(2a_j)^{N_f-N/2} c_j^N \\
&\quad \times \sum_{l_1} \frac{(-)^{l_f}}{\sqrt{2l_f+1}} (l'l00|l_1 0)(l_i l_1 m_i m_1|l_f m_f) W(l_i l_f l' l; l_1 l'') Y^*_{l_1 m_1}(\hat{\mathbf{r}}) \,,
\end{aligned} \tag{14}$$

where $R_{N,l}(r;\gamma)$ is the radial part of harmonic-oscillator wave function with oscillator-size parameter γ and the summation with respect to l runs $N_f - N, N_f - N - 2, \ldots, 0$ or 1, etc.

III. PION ELASTIC AND INELASTIC SCATTERING

The ground state of ^{7}Li has a large quadrupole deformation. It is, therefore, necessary to take into account the multipole scattering effect in pion-^{7}Li elastic scattering. Gibson *et al.* [8] assumed the DWIA and the strong-coupling rotational model for the ground and the first excited states. Then the monopole contribution to the elastic-scattering cross section is obtained by subtracting the inelastic-scattering cross section $^7\mathrm{Li}(\frac{3}{2}^- \rightarrow \frac{1}{2}^-;0.478\ \mathrm{MeV})$ from the experimental data of the elastic scattering. But it is not obvious whether DWIA is a good approximation or not to calculate the quadrupole effects in the elastic scattering.

Instead, we have calculated the multipole contribution explicitly by extending the optical potential to nonspherical nuclei. Due to its large quadrupole deformation of ^{7}Li, we expect that the coupling of the pion partial waves induced by quadrupole deformation is important. In order to take into account this coupling effect, we expanded the pion-nucleus wave function as

$$\Psi^{(+)}(\mathbf{k}\alpha : II_z) = 4\pi \sum_{l,m,J,J_z} i^l R_l^J(r) Y_{lm}^*(\hat{\mathbf{k}}) (lImI_z|JJ_z)[Y_l \otimes \Phi_I]^{JJ_z} \zeta_\alpha \ , \tag{15}$$

where $\mathbf{k}$ is the momentum, ζ_α the isospin wave function of the incident pion, and Φ_I is ^{7}Li ground-state wave function with spin I. The radial parts of the pion wave function $R_l^J(r)$ satisfy the coupled equation

$$\left[\frac{d^2}{dr^2} + \frac{2}{r}\frac{d}{dr} - \frac{l(l+1)}{r^2} + k^2\right] R_l^J(r) = 2\omega_\pi \left(\sum_{l'} U_{ll'}^J R_{l'}^J(r) + V_C R_l^J(r)\right) \ , \tag{16}$$

here $\omega_\pi = \sqrt{k^2 + m_\pi}$ is the pion total energy and V_C the pion-nucleus Coulomb potential. The pion-nucleus optical potential consists of monopole and multipole parts. For the monopole part, we adopted the optical potential by Stricker *et al.* [19–21] (MSU potential) which was extensively applied to the low-energy pion-nucleus scattering. Since we are concerned with the energy region T_π = 130–160 MeV, we have to extrapolate the absorption parameters B_0 and C_0 to higher energy. We adopted the parameters determined by Gmitro *et al.* [22]. Their approach is somewhat different from that of Stricker *et al.* The first-order optical potential is supplemented by the phenomenological ρ^2 terms which simulate the pion absorption and the higher-order effects. The coefficients B_0 and C_0 for these ρ^2 terms are determined from fit to the experimental data of the pion-nucleus elastic scattering. They obtained the energy-dependent parameters which are almost independent of the mass number of the target nucleus at $4 \leq A \leq 40$. At low-energy region, their parameters are close to the values of MSU potential. Gmitro *et al.* used the separable form for the off-shell extrapolation of the pion-nucleon scattering amplitude which is different from that of MSU potential. Generally speaking, however, the elastic- and the inelastic-scattering cross sections are rather insensitive to the off-shell model of the optical potential.

We constructed the quadrupole part of the optical potential under the first-order approximation

$$U_{ll'}^J = \left\langle [Y_l \otimes \Phi_I]^J \left| \sum_{j=1}^A t_j \right| [Y_{l'} \otimes \Phi_I]^J \right\rangle . \tag{17}$$

Here t_j is the scattering amplitude between pion and the jth nucleon, and is given approximately by the free pion-nucleon scattering amplitude. It is sufficient to take terms up to p wave:

$$t_j = -4\pi \frac{1}{2\bar{\omega}} \sum_{k=0,1} [b^{(k)} + c^{(k)} \mathbf{k}_f \cdot \mathbf{k}_i + id^{(k)} \boldsymbol{\sigma}_j \cdot (\mathbf{k}_f \times \mathbf{k}_i)] \times (\boldsymbol{\tau} \cdot \mathbf{T})^{(k)} \delta(\mathbf{r} - \mathbf{r}') \ . \tag{18}$$

The coefficients $b^{(k)}$, $c^{(k)}$, and $d^{(k)}$ are expressed in terms of the pion-nucleon phase shifts and $\bar{\omega}$ is the reduced energy of the pion [19]. We adopted the phase shifts in Ref. [23]. The momentum variables in Eq. (18) are replaced by the derivative operator acting on the pion wave function. The explicit form of the multipole terms in the optical potential is found in Ref. [34]. The pion partial waves couple through the multipole densities. In particular, the large quadrupole density strongly couples the pion partial waves l and $l \pm 2$ and this gives appreciable effects for the elastic-scattering cross section. The coupled differential equation Eq. (16) is solved numerically under suitable boundary condition.

The results of the elastic-scattering cross section are shown in Fig. 2 and are compared with the experimental data. For the case of T_π = 134 MeV, the elastic- and the inelastic-scattering cross section to first excited state are not separately measured. The results for T_π = 134 MeV are, therefore, the sum of these transitions. The dotted lines indicate the monopole contribution. As is seen, the contribution from quadrupole scattering becomes to be appreciable around the scattering angle $\theta \geq 60°$. We also showed the results obtained by switching off the coupling of partial waves. The coupling of the pion partial waves considerably enhances the cross section around the backward direction and it is necessary to take into account this effect properly for the case of the pion elastic scattering from deformed nucleus. In the present cluster-model calculation we neglected the spin-orbit interaction and, therefore, the quadrupole density of the ground state and the quadrupole spin-nonflip transition density have a simple relation. Neglecting the small spin-dependent matrix element and assuming DWIA, the quadrupole scattering contribution to the elastic scattering is given by the inelastic-scattering cross section leading to first excited state which is similar to the case of rotational model

[8]. But our results of the full calculation differ considerably from that of DWIA for the elastic-scattering cross section. It was shown that the DWIA and the optical potential treatment give almost the same results for the spin-flip amplitude in pion-^{13}C scattering [5] and this is due to the weak spin-dependent interaction in pion scattering. In contrast to this, the quadrupole effects are fairly strong and the DWIA is not sufficient and the treatment of the optical potential is necessary including the partial-wave coupling. We examined the sensitivity of the elastic-scattering cross section by slightly changing the parameters B_0 and C_0 for ρ^2 terms. But the results are quite insensitive to it.

Next we show the results of the inelastic-scattering cross section leading to the first excited state. In DWIA treatment, the inelastic transition amplitude can be given by

$$T_{fi} = \left\langle \Phi_{I'}\phi_f^{(-)} \left| \sum_j t_j \right| \Phi_I \phi_i^{(+)} \right\rangle , \qquad (19)$$

where Φ_I and $\Phi_{I'}$ are initial and final states for nucleus. $\phi_i^{(+)}$ and $\phi_i^{(-)}$ are the incident and outgoing pion wave functions, respectively.

The effects concerning the nuclear structure are included in the spin-nonflip ($\rho_{fi}^{(k)}$) and the spin-flip ($\boldsymbol{\rho}_{fi}^{(k)}$) transition densities. These are given by

$$\left\{ \begin{array}{c} \rho_{fi}^{(k)}(\mathbf{r}) \\ \boldsymbol{\rho}_{fi}^{(k)}(\mathbf{r}) \end{array} \right\} = \left\langle f \left| \sum_j \left\{ \begin{array}{c} 1 \\ \boldsymbol{\sigma}_j \end{array} \right\} \tau_3^{(k)}(j)\delta(\mathbf{r} - \tilde{\mathbf{r}}_j) \right| i \right\rangle . \qquad (20)$$

In the practical calculation, we have carried out the multipole expansion of the inelastic transition amplitude as in Ref. [35]. The pion distorted waves are generated by the pion-nucleus optical potential with spherical part only. The results are shown in Fig. 3 for T_π = 143 and 164 MeV. In the inelastic transition ^{7}Li$(\pi,\pi')^7$Li$(\frac{1}{2}^-$:0.478 MeV), the spin-nonflip quadrupole contribution dominates the cross section and we obtained a good agreement with the experimental data without introducing effective charges. As was shown in Ref. [8], the simple collective-model description fails badly to explain the experimental data: the theoretical values are about an order of magnitude smaller than the experiment at backward direction. The results calculated with the shell model are also shown in Fig. 3. We used the Cohen-Kurath wave function with (8–16) POT two-body matrix elements [36]. If we introduce the quadrupole effective charges [37], the agreement with the experimental data becomes much better than the collective model. The theoretical value, however, still slightly underestimates the cross section especially at backward direction. In order to see the size effect of the clusters, we have calculated the extreme case with the oscillator-size parameters $\nu_\alpha = \nu_t = 0.32$ fm^{-2} which was examined by Kajino *et al.* [17]. Figure 4 shows the cluster-size dependence of the pion inelastic-scattering cross section. Obviously, the cluster-size effect becomes to be appreciable

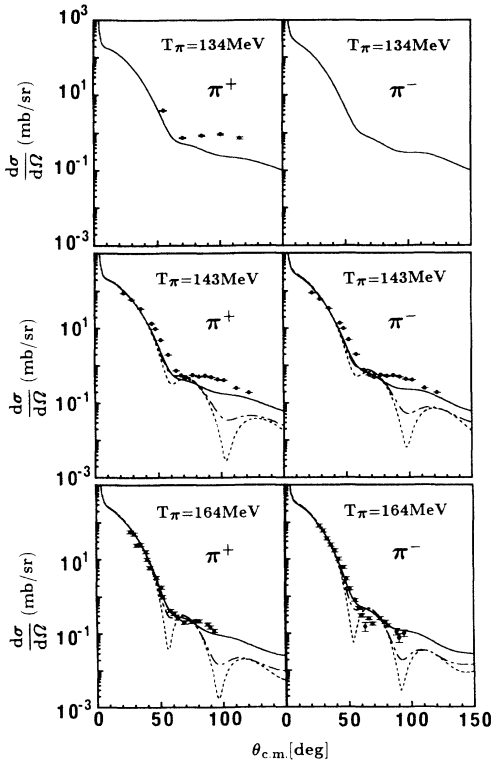

FIG. 2. Pion elastic-scattering cross sections from ^{7}Li. The monopole contribution (dotted lines) and the results of the full calculation with quadrupole densities (solid lines) are shown. The dash-dotted lines are the results calculated by switching off the coupling of the pion partial waves induced by quadrupole deformation. For the case of T_π = 134 MeV, the inclusive cross section leading to ground plus first excited states are shown. The experimental data are taken from Refs. [1–3].

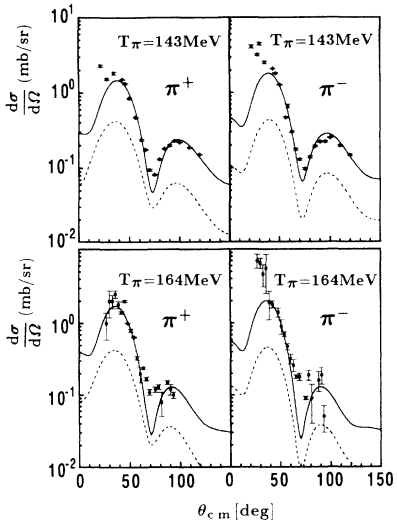

FIG. 3. Inelastic-scattering cross section leading to the first excited state ^{7}Li$(\pi^\pm,\pi^\pm)^7$Li$(\frac{1}{2}^-$:0.478 MeV). The solid lines are the results with the cluster-model wave function. The dotted lines are obtained by the shell model without using effective charges. The experimental data are taken from Refs. [1,2].

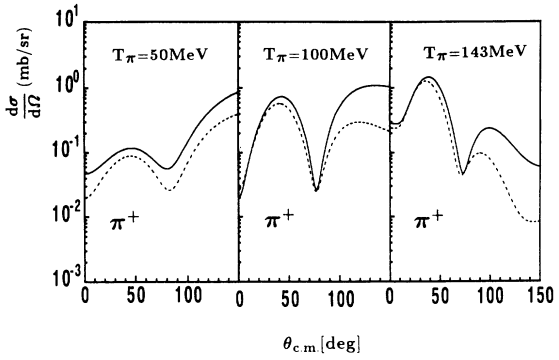

FIG. 4. The cluster-size effects for the pion inelastic scattering ^{7}Li$(\pi^\pm,\pi^\pm)^7$Li$(\frac{1}{2}^-$:0.478 MeV). The solid lines are the results with oscillator-size parameters $\nu_\alpha = 0.546$ fm^{-2} and $\nu_t = 0.413$ fm^{-2}. The dotted lines correspond to the results with size parameters $\nu_\alpha = \nu_t = 0.32$ fm^{-2}.

around the large-q region.

For the polarization observables, we compare the results with the second-rank tensor polarization Θ_{zz} defined by

$$\Theta_{zz} = -\tfrac{1}{2}T_{20} - \sqrt{3/2}T_{22}\ , \tag{21}$$

where we adopted the Madison convention [38]. The results are shown in Fig. 5. In the recent experiment at PSI [9,39], the final spin-doublet states are not separately observed. Hence, we took the average of the polarization leading to ground and first excited states as

$$\Theta_{zz} = \frac{(d\sigma/d\Omega)(\text{g.s.})\Theta_{zz}(\text{g.s.}) + (d\sigma/d\Omega)(\frac{1}{2}^-)\Theta_{zz}(\frac{1}{2}^-)}{(d\sigma/d\Omega)(\text{g.s.}) + (d\sigma/d\Omega)(\frac{1}{2}^-)}\ . \tag{22}$$

Although the error of the experiment is fairly large and the detailed comparison is difficult, our results are not inconsistent with the experimental data. The second-rank tensor polarization Θ_{zz} just corresponds to the difference of the number of pions scattered by the target nucleus with spin projection $I_z = \frac{1}{2}$ and $I_z = \frac{3}{2}$, where the quantization z axis is chosen to be perpendicular to the scattering plane. In a classical picture, the symmetry axis of the pancake-shaped ^{7}Li is perpendicular to the scattering plane in the case of $I_z = \frac{3}{2}$ while the symmetry axis is in the scattering plane for $I_z = \frac{1}{2}$. It is, therefore, apparent that the quadrupole effects are appreciable for Θ_{zz} and it takes large absolute values for the deformed nuclei like ^{7}Li. It should be noted that the second-rank tensor polarization takes large absolute values even at forward direction where the reaction mechanism is simpler. Similar effects were used to extract the neutron deformation parameter from pion single-charge-exchange reaction on an aligned ^{165}Ho nucleus [6].

In the present paper we have not discussed about the vector polarization iT_{11}. Considering that the α-t cluster model is also successful in explaining the magnetic form factor of ^{7}Li, it would be interesting to study the vector polarization based on a cluster model and compare them with the results obtained with the shell-model calculation [9]. In this case, it should be stressed that we have to treat the quadrupole effects properly which are expected to influence the vector polarization. The calculation of the vector polarization is now under way.

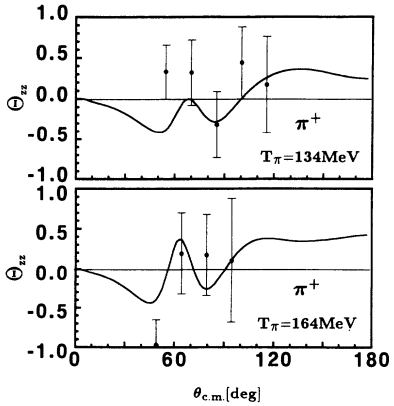

FIG. 5. The second-rank tensor polarization Θ_{zz} for the inclusive transition leading to ground plus first excited states of ^{7}Li. The experimental data are taken from Ref. [39].

IV. SUMMARY

We have investigated the quadrupole scattering effects in the pion elastic- and inelastic-scattering cross section for ground and first excited states of ^{7}Li. The RGM wave function with α-t configuration is employed for the ground and the first excited states of ^{7}Li, which is known to describe the electromagnetic properties quite well. We calculated the multipole part of the pion-nucleus optical potential under the first-order approximation while the monopole part is calculated by phenomenological MSU potential.

For the elastic-scattering cross section, it is found that the quadrupole effects are appreciably large, especially, for the backward angles ($\theta \geq 60°$). We also showed that the effect of the coupling of the pion partial waves induced through the quadrupole density is considerably large for such a deformed nucleus and that the proper treatment of the quadrupole effects is important.

For the inelastic transition to the first excited state, the spin-nonflip quadrupole contribution dominates the cross sections. It is to be noted that the experimental data can be well described without introducing the effective charges. If we use the shell-model wave function for ^{7}Li, it is necessary to introduce effective charges and still the theoretical value slightly underestimates the experimental cross section. The cluster-model wave function provides us with consistent description for the spin-doublet states.

We also compared our results with the recent experimental data of averaged second-rank tensor polarization Θ_{zz}. Though the detailed comparison is difficult due to the large experimental errors, the theoretical and experimental results are consistent. From the theoretical viewpoint, it is expected that the quadrupole effects are appreciably large in second-rank tensor polarization Θ_{zz} and that Θ_{zz} has large value even at forward angles.

ACKNOWLEDGMENTS

We are grateful to Dr. R. Meier for stimulating discussions. One of us (K.K.) would like to thank Professor H. W. Fearing and the member of the TRIUMF theory group for their hospitality during his stay at TRIUMF, where a part of this work was done.

[1] R. Tacik *et al.*, Phys. Rev. Lett. **63**, 1784 (1989).
[2] R. Meier *et al.*, Phys. Rev. C **42**, 2222 (1990).
[3] S. Ritt *et al.*, Phys. Rev. C **43**, 745 (1991).
[4] Yi-Fen Yen *et al.*, Phys. Rev. Lett. **66**, 1959 (1991).
[5] P. B. Siegel and W. R. Gibbs, Phys. Rev. C **48**, 1939 (1993).
[6] J. N. Knudson *et al.*, Phys. Rev. Lett. **66**, 1026 (1991).
[7] J. Bolger, E. Boschitz, R. Mischke, A. Nagel, W. Saathoff, C. Wiedner, and J. Zichy, in *Meson-Nuclear Physics-1979 (Houston)*, Proceedings of the 2nd International Topical Conference on Meson-Nuclear Physics, AIP Conf. Proc. No. 54, edited by E. V. Hungerford, III (AIP, New York, 1979), p. 519.
[8] E. F. Gibson, J. J. Kraushaar, T. G. Masterson, R. J. Peterson, R. S. Raymond, R. A. Risttinen, R. L. Boudrie, and N. S. P. King, Nucl. Phys. **A377**, 389 (1982).
[9] R. Meier *et al.* Phys. Rev. **49**, 320 (1994).
[10] D. A. Sparrow, Nucl. Phys. **A276**, 365 (1977).
[11] M. Bouten, M. C. Bouten, and P. van Leuven, Nucl. Phys. **A102**, 322 (1967); **A111**, 385 (1968).
[12] J. Kruger and P. van Leuven, Nucl. Phys. **A139**, 418 (1969).
[13] C. M. Chesterfield and B. M. Spicer, Nucl. Phys. **41**, 675 (1963).
[14] D. Kurath, Nucl. Phys. **14**, 398 (1960); **140**, B1190 (1965).
[15] H. Kanada, Q. K. K. Liu, and Y. C. Tang, Phys. Rev. C **22**, 813 (1980).
[16] H. Walliser, Q. K. K. Liu, H. Kanada, and Y. C. Tang, Phys. Rev. C **28**, 57 (1983).
[17] T. Kajino, T. Matsuse, and A. Arima, Nucl. Phys. **A413**, 323 (1984); **A414**, 185 (1984).
[18] M. Unkelbach and H. M. Hofmann, Phys. Lett. B **261**, 211 (1991).
[19] K. Stricker, H. McManus, and J. A. Carr, Phys. Rev. C **19**, 929 (1979).
[20] K. Stricker, J. A. Carr, and H. McManus, Phys. Rev. C **22**, 2043 (1980).
[21] J. A. Carr, H. McManus, and K. Stricker-Bauer, Phys. Rev. C **25**, 952 (1982).
[22] M. Gmitro, S. S. Kamalov, and R. Mach, Phys. Rev. C **36**, 1105 (1987).
[23] G. Rowe, M. Salomon, and R. H. Landau, Phys. Rev. C **18**, 584 (1978).
[24] A. B. Volkov, Nucl. Phys. **74**, 33 (1965).
[25] F. Ajzenberg-Selove, Nucl. Phys. **A320**, 1 (1979).
[26] G. J. C. van Niftrik, L. Lapikas, H. deVries, and G. Box, Nucl. Phys. **A174**, 173 (1971).
[27] H. Orth, H. Ackermann, and E. W. Otten, Z. Phys. A **273**, 221 (1975).
[28] S. L. Kahalas and R. K. Neset, J. Chem. Phys. **39**, 529 (1963).
[29] O. Häusser, A. B. McDonald, T. K. Alexander, A. J. Ferguson, and R. E. Warner, Phys. Lett. **38B**, 75 (1972).
[30] J. Lichtenstadt, M. A. Moinester, J. Dubach, R. S. Hicks, G. A. Peterson, and S. Kowalski, Phys. Lett. B **219**, 394 (1989).
[31] J. Janssens, R. Hofstadter, E. B. Hughes, and M. R. Yearian, Phys. Rev. **142**, 922 (1966).
[32] A. Hasegawa and S. Nagata, Prog. Theor. Phys. **45**, 1786 (1971).
[33] K. Ikeda, R. Tamagaki, S. Saito, H. Horiuchi, A. Tohsaki-Suzuki, and M. Kamimura, Prog. Theor. Phys. Suppl. **62** (1977).
[34] K. Kume, Phys. Lett. **106B**, 271 (1981).
[35] T. Nishiyama and H. Ohtsubo, Prog. Theor. Phys. **52**, 952 (1974).
[36] S. Cohen and D. Kurath, Nucl. Phys. **73**, 1 (1965).
[37] A. G. M. van Hees and P. W. M. Glaudemans, Z. Phys. A **315**, 223 (1984).
[38] *Proceedings of the 3rd International Symposium on Polarization Phenomena in Nuclear Reactions*, edited by H. H. Barschall and W. Haeberli (The University of Wisconsin Press, Wisconsin, 1971), p. xxv.
[39] R. Meier, Ph.D. thesis, University of Karlsruhe, 1993.